Available online at www.sciencedirect.com

ScienceDirect

Ceramics International 40 (2014) 2441–2450

CERAMICS INTERNATIONAL

www.elsevier.com/locate/ceramint

Structural and electrical properties of sodium bismuth titanate ($Na_{0.5}Bi_{0.5}TiO_3$) thin films optimized using the Taguchi approach

A.S. Daryapurkar[a,*], J.T. Kolte[a], P.R. Apte[b], P. Gopalan[a]

[a]Department of Metallurgical Engineering & Materials Science, Indian Institute of Technology Bombay, Powai, Mumbai 400076, India
[b]Department of Electrical Engineering, Indian Institute of Technology Bombay, Powai, Mumbai 400076, India

Received 19 June 2013; received in revised form 5 August 2013; accepted 5 August 2013
Available online 15 August 2013

Abstract

Controllable Pulsed Laser Deposition (PLD) parameters have been optimized to grow sodium bismuth titanate ($Na_{0.5}Bi_{0.5}TiO_3$) (NBT) thin films. Target to substrate distance, background gas pressure, substrate temperature, laser fluence, laser rate of repetition, annealing time and NBT targets with and without excess Bi have been chosen as the parameters using a Taguchi L_{18} orthogonal array. Taguchi's Signal-to-Noise (S/N) ratios and analysis of variance (ANOVA) tools highlight the relevance of each parameter, and also yield the optimal setting of the parameters. The dominant parameters affecting dielectric properties are oxygen gas pressure and substrate temperature, whereas the distance between target to substrate and laser fluence appear as significant parameters. Fine tuning experiments and a subsequent verification experiment using the dominant and significant parameters result in the best values for the dielectric constant of 735, dielectric loss of 0.07 at 1 kHz and remnant polarization of 21.42 μC/cm^2.

Keywords: A. Films; C. Dielectric properties; C. Ferroelectric properties; Pulsed Laser Deposition; Taguchi method

1. Introduction

Now a days, several research groups are putting efforts to replace lead based materials by lead free materials because of their environmental impact. More environmentally benign compounds such as sodium bismuth titanate ($Na_{0.5}Bi_{0.5}TiO_3$) known as NBT have therefore been attracting attention as a lead-free ferroelectric material. NBT exhibits a higher Curie temperature (320 °C) and excellent dielectric characteristics thereby making it a prospective candidate as an environment friendly material. Investigations on bulk NBT justify the demand for thin film studies leading to devices applications. A number of investigations have focused on NBT thin films [1–9]; invariably stoichiometry has been achieved only where excess Na and/or Bi have been used. Tang et al. [3] have reported on the preparation and electrical properties of highly (111) oriented NBT thin films by a sol–gel process with the precursor containing 10% excess Bi. On the other hand, Yu et al. [5] have deposited NBT thin films using 10 mol% excess Na in the solution. Duclere et al. [8] have deposited NBT thin films by PLD on an epitaxial (1 1 1) Pt layer supported by a c-sapphire substrate using 20 mol% excess Na and Bi. Despite the Na and Bi excess in the target, a secondary phase has been observed in the XRD pattern. Further, they have cited the need to optimize the pulsed laser deposition (PLD) growth parameters. Bousquet et al. [9] have also studied the dielectric and ferroelectric properties of NBT thin film grown by PLD using excess Na and Bi target. They have also reported the need to optimize the PLD parameters to reduce the density of grain boundaries and the elimination of the secondary phase.

It is well known that the quality of the oxide thin films significantly depend on the PLD growth parameters, namely target to substrate distance, ambient gas pressure, substrate temperature, laser fluence, laser rate of repetition, annealing time and target composition. It has been reported that the best quality of the thin film has been achieved when the substrate is at the extremity of the plume. Irregular and rough surface morphologies have been observed at the shorter distance due to excessive bombardment of plasma species at the substrate surface. Ambient oxygen gas pressure plays an important role

*Corresponding author. Tel.: +91 22 2576 4657, mobile: +91 9867245331; fax: +91 22 2572 6975.
E-mail address: asdaryapurkar@iitb.ac.in (A.S. Daryapurkar).

0272-8842/$ - see front matter © 2013 Elsevier Ltd and Techna Group S.r.l. All rights reserved.
http://dx.doi.org/10.1016/j.ceramint.2013.08.019

to maintain the stoichiometry and the oxygen vacancies in the thin film. Substrate temperature plays crucial role in the composition, structure, crystalline quality, and the texture characteristics of the films. In case of fixed laser wavelength for a particular material, laser fluence on the target has significant effect on the particulate size and density of the thin films. Above the threshold laser fluence, the particulate number density increases rapidly with increasing fluence. However, it reduces at higher fluence due to saturation in the ablation process. Continuous and uniform thin films can be achieved at optimum laser rate of repetition. Moreover, it helps to avoid the deficiency of volatile species with controlling evaporation rate of the material. Annealing temperature and duration have negligible effect on the structure and properties of the thin films which can be compensate using optimum deposition temperature. Target composition has important role when it contains volatile elements such as Pb, Bi, K and Na [10–14]. Deposition of single phase NBT thin film is the challenge since the composition consists of volatile components such as Na and Bi. To get the single phase, good quality NBT thin film, systematic study of optimization of PLD parameters is required. In this work, Taguchi's approach has been used to optimize the PLD control parameters. Obtaining good structural and electrical properties in a single phase NBT thin film is the goal of our optimization strategy.

2. Experimental details

2.1. Taguchi method

Design of Experiment (DoE) is a powerful statistical technique for determining the optimum settings of the control factors to make a process insensitive to noise factors. In a trial and error approach, characterization has to be carried out following every film growth so that an analysis of observed data will help decide the extent and the variation in each parameter. Further, the data is usually insufficient to draw any significant conclusion. On the other hand, Taguchi approach offers many benefits which are based on “Orthogonal Array”. First, it comprises a set of well-balanced minimum experiments and the conclusion arrived from such experiments are valid over the entire experimental region spanned by the control factors and their settings. Second, there is large saving in the experimental efforts. Third, the data analysis is easy. For example, for the case of one parameter at two levels and seven parameters at three levels, the Taguchi approach reduces the number of experiments from about 4374 ($2^1 \times 3^7$) to 18. Chou et al. [15] have used the Taguchi experimental design to optimize the processing parameters of hollow cathode discharge ion-plating and unbalanced magnetron sputtering to deposit ZrN and TiN thin film on Si (100) substrate. Also, the Taguchi method with a L_9 orthogonal array has been employed by Hsu et al. [16] to optimize the processing parameters of radio frequency magnetron sputtering. Also, Cheng et al. [17] have adopted Taguchi method to optimize the control parameters of modified chemical vapor deposition for growing TiO_2 thin films.

Taguchi method involves eight steps that can be grouped into three major categories of planning experiments, conducting them, and analyzing and verifying the results.

2.1.1. Planning the experiments

2.1.1.1. Identify the main function, side effects and failure mode. There are several problems in PLD deposited NBT thin films, namely non-uniformity of thin film on large area, roughness, and defects like pinholes, particulates that can deteriorate the dielectric and ferroelectric properties.

2.1.1.2. Identify noise factors and the testing conditions for evaluating the quality loss. Two types of noise factors exist in the deposition process. External noise factors like temperature and humidity are difficult and expensive to control. Others are internal noise factors include substrate handling and cleaning, variation in thickness and roughness of thin films due to position of substrate on substrate holder, topography of the wafer surface before deposition, variation in gas supply and status of gas cylinder through which gas is supplied. To minimize sensitivity to noise factors, two sets of thin films have been deposited with same parameters. Thereafter, electrodes of Cr–gold having 500 μm diameter have been deposited on each sample by thermal evaporation method using shadow mask. Dielectric measurements have been undertaken on these samples.

2.1.1.3. Identify the quality characteristic to be observed and the objective function to be optimized. There are two quality characteristics of interest, namely dielectric constant and dielectric loss. The two quality characteristics have their corresponding objective function, also called as signal-to-noise (S/N) ratio, defined in Eqs. (1) and (2) (see Section 2.2).

2.1.1.4. Identify the control factors and their alternate levels. In this work, L_{18} orthogonal array has been designed with one 2-level and six 3-level parameters. The seven parameters are distance between target to substrate (A), background oxygen gas pressure (B), substrate temperature (C), laser fluence (D), laser pulse rate (E), annealing time (F), and pure and excess Bi containing targets (G). One parameter has been left empty; the Taguchi method permits such a choice. These parameters with their levels are listed in Table 1.

2.1.1.5. Design the matrix experiment and define the data analysis procedure. In this experiment, modified L_{18} orthogonal array has 7 columns and 18 rows. The 18 rows in Table 2 for L_{18} array represent the 18 experiments that are to be conducted. Combination of parameters and number of experiments are given in Table 2.

2.1.2. Performing the experiments

2.1.2.1. Conduct the matrix experiment and data collection. Experiments have been performed using the combination of parameters as given in Table 2. To achieve a fixed film thickness of 400 nm, 8000 laser shots have been used in each

Table 1
Control factors and their levels.

Sr. no.	Factors	Levels		
		1	2	3
1	Distance between target to substrate (cm)	4	4.5	
2	Oxygen pressure (mbar)	0.1	0.3	0.5
3	Substrate temperature (°C)	550	600	650
4	Laser fluence (J/cm^2)	1.5	2	2.5
5	Rate of repetition (Hz)	2	5	10
6	Target	NBT	NBT10	NBT30
7	Annealing time ($_{min}$)	No	15	30
8	Empty	–	–	–

Table. 2
L18 orthogonal array.

Samples name	Control factors assigned to columns						
	Distance between target to substrate (cm)	Oxygen pressure (mbar)	Substrate temperature (^{o}C)	Laser fluence (J/cm^2)	Rate of repetition (Hz)	Target	Annealing time ($_{min}$)
Sample 1	4	0.1	550	1.5	2	NBT	None
Sample 2	4	0.1	600	2	5	NBT10	15
Sample 3	4	0.1	650	2.5	10	NBT30	30
Sample 4	4	0.3	550	1.5	5	NBT10	30
Sample 5	4	0.3	600	2	10	NBT30	None
Sample 6	4	0.3	650	2.5	2	NBT	15
Sample 7	4	0.5	550	2	2	NBT30	30
Sample 8	4	0.5	600	2.5	5	NBT	None
Sample 9	4	0.5	650	1.5	10	NBT10	15
Sample 10	4.5	0.1	550	2.5	10	NBT10	None
Sample 11	4.5	0.1	600	1.5	2	NBT30	15
Sample 12	4.5	0.1	650	2	5	NBT	30
Sample 13	4.5	0.3	550	2	10	NBT	15
Sample 14	4.5	0.3	600	2.5	2	NBT10	30
Sample 15	4.5	0.3	650	1.5	5	NBT30	None
Sample 16	4.5	0.5	550	2.5	5	NBT30	15
Sample 17	4.5	0.5	600	1.5	10	NBT	30
Sample 18	4.5	0.5	650	2	2	NBT10	None

deposition. Dielectric constant and dielectric loss of the Au/NBT/Pt capacitor has been measured in the frequency range from 1 kHz to 1 MHz at room temperature using "Broad Band Dielectric Spectrometer" (Novocontrol concept 80 systems, GmbH, Germany). Data at 1 MHz has been used to analysis using analysis of variance (ANOVA) to obtain the best setting of parameters.

Fig. 1 exhibits the dielectric constant for samples 1–9 while Fig. 2 exhibits the dielectric constant for samples 10 to 18. The dielectric constant decreases slowly over the frequency range from 1 kHz to 1 MHz. Maximum samples have a dielectric constant less than 500 at 1 kHz. However, sample 12 exhibits a higher dielectric constant which is around 700 along with the large dispersion of dielectric constant over the frequency range. Sample 8 exhibits lower dielectric constant compared to all other samples.

Figs. 3 and 4 exhibit the dielectric loss for samples 1–9 and 10–18 respectively. Dielectric loss is higher at lower frequency and it is decreases slowly over the frequency range. Majority of the samples have dielectric loss in the range 0–0.5. Among all samples, sample 2 exhibits good dielectric properties. It has a dielectric constant and dielectric loss of 520 and 0.085 respectively.

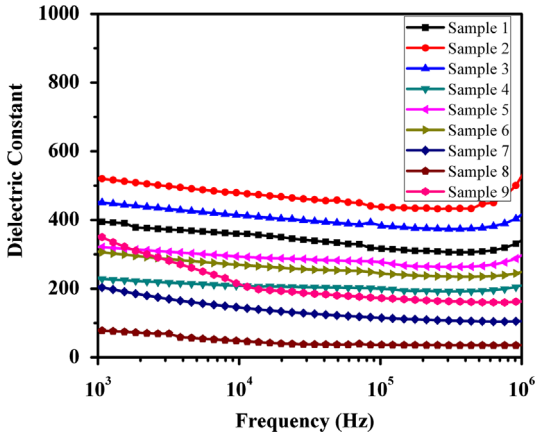

Fig. 1. Dielectric constant of NBT thin films as a function of frequency for samples 1–9.

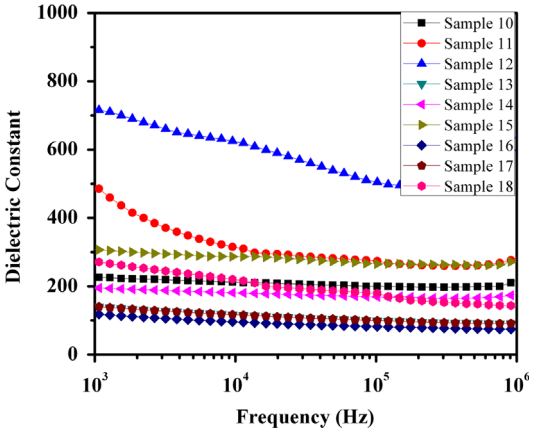

Fig. 2. Dielectric constant of NBT thin films as a function of frequency for samples 10–18.

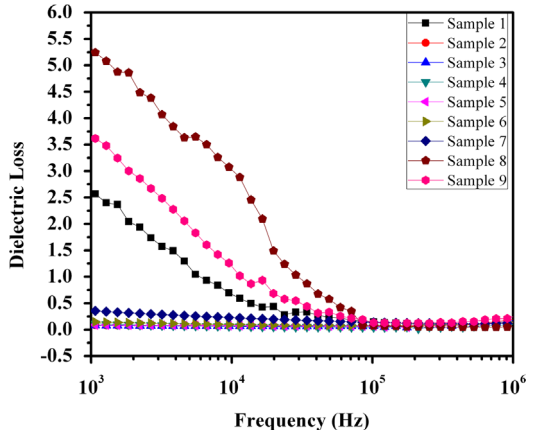

Fig. 3. Dielectric loss of NBT thin films as a function of frequency for samples 1–9.

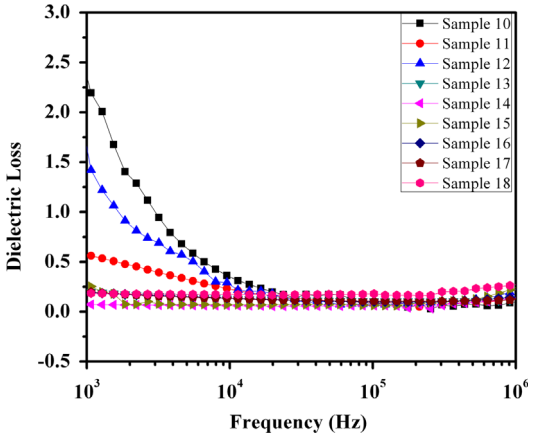

Fig. 4. Dielectric loss of NBT thin films as a function of frequency for samples 10–18.

2.2. Statistical calculations

Analysis of Variance (ANOVA) has been used to determine the influence of every parameter on the variance of the results. The method involves the Signal-to-Noise ratios (S/N) that are logarithmic functions of the desired output. These S/N ratios serve as a objective function for optimization and are used in data analysis as well as prediction of optimum results. The detailed review on the calculation of percentage factor effects and ANOVA can be found in the reference [18]. Calculation of the S/N ratio depends on the experimental objective, such as "larger the better" for dielectric constant and "smaller the better" for dielectric loss. It is defined as,

$$\eta_i = -10\log_{10}(\text{mean square reciprocal of dielectric constant}) \quad (1)$$

$$\eta_i = -10\log_{10}(\text{mean square of dielectric loss}) \quad (2)$$

Where, i is the total number of experiments.

The overall mean value (m) of η for 18 experiment is defined as,

$$m = [(\eta_1 + \eta_2 + \cdots + \eta_{18})/18] \quad (3)$$

The effect of factor level is defined as the deviation it causes from the overall (OV) mean. Let us consider the example of evaluating effect of distance between target to substrate at the first level, i.e. 4 cm which is presented in the experiments 1–9. The average S/N ratio for these experiments, denoted by m_{A1}, is given by,

$$m_{A1} = [(\eta_1 + \eta_2 + \eta_3 + \eta_4 + \eta_5 + \eta_6 + \eta_7 + \eta_8 + \eta_9)/9] \quad (4)$$

Similarly, the average S/N ratio for second level of distance between target to substrate, i.e. 4.5 cm is given by,

$$m_{A1} = [(\eta_{10} + \eta_{11} + \eta_{12} + \eta_{13} + \eta_{14} + \eta_{15} + \eta_{16} + \eta_{17} + \eta_{18})/9] \quad (5)$$

The average S/N ratio for all levels of all parameters can be obtained in a similar manner. The average η for each level of the seven parameters has been tabulated in Tables 3 and 4. These averages are shown graphically in Figs.5 and 6.

There are nine experiments each at the first and second level for parameter A. The sum of squares due to parameter A is defined as,

$$\text{Sum of square due to parameter } A = 9[(m_{A1} - m)^2 + (m_{A2} - m)^2] \quad (6)$$

$$\text{Total sum of squares} = (\text{sum of the sums of squares due to factors } A, B, C, D, E, F \text{ and } G) \quad (7)$$

$$\text{Mean square} = (\text{Sum of square})/(\text{Degree of freedom}) \quad (8)$$

Where, degree of freedom associated with a factor is one less than the number of levels of parameter.

$$\text{Percentage factor effect} = [9(\text{Sum of square}/\text{Total sum of square}) \times 100] \quad (9)$$

All the values of degree of freedom, sum of squares, mean square, and percentage factor effect have been tabulated in Tables 3 and 4 (see Section 3.1).

The L_{18} array detailing the experiments performed along with the values for the control parameters are listed in Table 2. The outcome of these experiments has been analyzed for optimization

Table. 3
ANOVA table for dielectric constant.

Control factors	Average η' by level (dB)			Degrees of freedom	Sum of squares	Mean square	Factor effect (percent)	Contribution of selected level to S/N ratio (in dB)	Dominant or significant or negligible	Optimum level
	1	2	3							
Distance between target to substrate	49.88	46.86		1	41	41	**14**	1.51	**Significant**	4 [cm]
Oxygen Pressure	52.15	46.48	46.48	2	129	64	**44**	3.78	**Dominant**	0.1 [mbar]
Distance between T-S (1) and Pressure (1,2,3)	−0.63	0.32	0.32	2	4	2	**1**			
Distance between T-S (2) and Pressure (1,2,3)	0.63	−0.32	−0.32							
Substrate temperature	45.87	48.61	50.64	2	69	34	**23**	2.27	**Dominant**	650 [°C]
Laser fluence	48.44	49.27	47.41	2	10	5	**4**	0.00	**Negligible**	—
Rate of repetition	49.13	49.16	46.83	2	21	11	**7**	0.79	**Significant**	5 [Hz]
Target	48.25	48.40	48.47	2	0	0	**0**	0.00	**Negligible**	– –
Annealing time	49.40	47.98	47.74	2	10	5	**3**	0.00	**Negligible**	–
Range for dielectric constant=471–996						Predicted dielectric constant=685				

of the dielectric constant and dielectric loss. The predictions of the analysis yield a "best setting" of the parameters, resulting in maximum dielectric constant coupled with the minimum dielectric loss.

3. Results and discussion

3.1. Taguchi analysis

3.1.1. Analyzing and verifying the experiment results

3.1.1.1. Analyze the data, determine optimum levels for the control factors and predict the performance under these levels. Fig. 5 depicts the factor effect plot for dielectric constant. The optimum level for each parameter refers to the highest value of S/N ratio. The best setting for highest dielectric constant has been selected from Fig. 5 and data tabulated in Table 3.The effect of the parameters based on their contribution to the dielectric properties (percentage factor effect = X), have been labeled as dominant ($X > 15$), significant ($5 \leq X \leq 15$), and negligible ($X < 5$).

From Fig. 5 and Table 3, it is observed that oxygen pressure and substrate temperature are dominant parameters that have 44% and 23% factor effect on the dielectric properties respectively. These parameters play an important role in improving the dielectric constant whereas distance between target and substrate and pulse rate of repetition play a significant role, and have 14% and 7% factor effect respectively. The remaining three parameters namely laser fluence, NBT target and annealing time have negligible effect. From Taguchi analysis, for larger dielectric constant, the best distance between target and substrate is 4 cm; the best oxygen pressure is 0.1 mbar; the best substrate temperature is 650 °C; and the best setting for pulse repetition rate is 5 Hz. Fine tuning and verification experiments are predicted to yield a dielectric constant value of 685 while the range for the value calculated using additivity model is expected to be between 471 and 996.

Similarly, the factor effect plot and analysis of variance (ANOVA) were also followed for dielectric loss. Fig. 6 depicts factor effect plot for dielectric loss. Best settings for smaller dielectric loss have been selected from Fig. 6 and ANOVA Table 4.

It is observed that oxygen pressure, substrate temperature and pulse rate of repetition are dominant parameters with 22%, 30%, and 19% factor effect respectively. These parameters play an important role to improve the dielectric loss whereas laser fluence and annealing time play significant role and have 11% factor effect. The remaining two parameters namely distance between target to substrate and NBT target have been found to have negligible effect. Thus, for the dielectric loss, the best setting for oxygen pressure is 0.3 mbar; the best substrate temperature is 650 °C; the best setting for pulse repetition rate is 5 Hz and the best setting for annealing time is 30 min. The predicted dielectric loss from the fine tuning and verification experiments is about 0.010 while the predicted range for the same is between 0.032 and 0.003. All dominant parameters have been considered for selecting the best setting

Table. 4
ANOVA table for dielectric loss.

Control factors	Average η' by Level (dB)			Degrees of freedom	Sum of squares	Mean square	Factor effect (percent)	Contribution of selected level to S/N ratio (dB)	Dominant or significant or negligible	Optimum level
	1	2	3							
Distance between target to substrate	13.05	13.59		1	1	1	**0**	0	**Negligible**	–
Oxygen pressure	6.14	19.49	14.34	2	544	272	**22**	6.17	**Dominant**	0.3 [mbar]
Distance between T-S (1) and pressure (1,2,3)	0.53	−0.26	−0.27	2	3	1	0			
Distance between T−S (2) and pressure (1,2,3)	−0.53	0.26	0.27							
Substrate temperature	4.13	17.98	17.85	2	760	380	**30**	4.66	**Dominant**	650 [°C]
Laser fluence	7.80	17.15	15.01	2	288	144	**11**	3.83	**Significant**	2 [J/cm^2]
Rate of repetition	8.29	20.43	11.24	2	481	241	**19**	7.11	**Dominant**	5 [Hz]
Target	12.18	12.04	15.75	2	53	27	**2**	0.00	**Negligible**	–
Annealing time	8.68	13.16	18.12	2	267	134	**11**	4.80	**Significant**	30 min
Range for dielectric loss=0.032–0.003						Predicted dielectric loss=0.010				

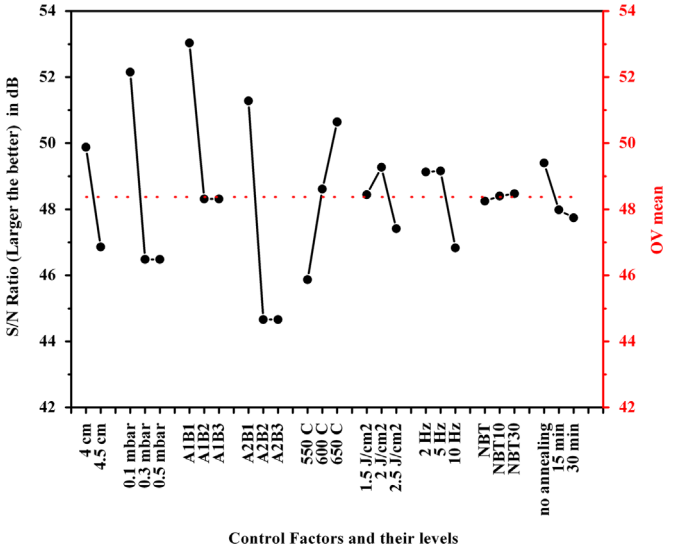

Fig. 5. Factor effect plot for dielectric constant.

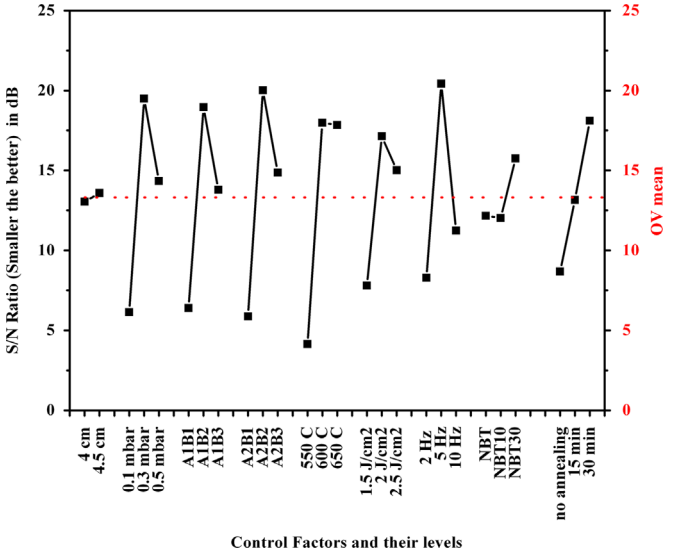

Fig. 6. Factor effect plot for dielectric loss.

to obtain a large dielectric constant and low dielectric loss with respect to their percentage of factor effect provided in Table 5.

The task of determining the best setting of each control factor for two different properties is complicated. This is because different levels of the same parameter can be optimum for the two properties. Hence, dielectric constant has been considered as the more important property for deciding the best settings of the parameters. The best setting of the distance between target to substrate is 4 cm which yields a large improvement in the dielectric constant with negligible effect on dielectric loss as shown in Figs. 5 and 6. A compromise in the selection of pressure is required to obtain high dielectric constant with low dielectric loss. 0.3 mbar has been selected as it shows large improvement (7 dB from over all mean) in dielectric loss as shown in Fig.6. However, the same setting of 0.3 mbar shows only a slight degradation (2 dB from over all

mean) in dielectric constant as shown in Fig. 5. Interaction between controls factors namely, *A* (distance between target and substrate) and *B* (oxygen background gas pressure) is shown in Fig. 5 and Fig. 6 as (*A*1*B*1, *A*1*B*2, *A*1*B*3) and (*A*2*B*1, *A*2*B*2, *A*2*B*3). It can be seen that these curves are parallel, indicating that there is no interaction between the two control factors. Therefore, the best settings of *A* and *B* can be selected on the basis of improvement of dielectric constant and/or dielectric loss as has been done above. The best substrate temperature is 650 °C; the best laser fluence is 2 J/cm^2; and the best pulse repetition rate is 5 Hz. Target and annealing time shows negligible effect on dielectric constant as shown in factor effect plot for dielectric constant (Fig. 5), hence NBT target without excess and no annealing time has been chosen as a best level. The last row in Table 5 gives the best setting of all dominant parameters.

3.1.1.2. Conduct the fine tuning and verification experiment. From the Taguchi analysis it is noted that the substrate temperature and oxygen pressure are the dominant parameters which crucially affect the surface morphology, structural and dielectric properties of NBT thin films. During experiments, it is observed that the crystallinity and grain size of the thin film increases with the temperature consequently there is improvement in the dielectric properties. It is well known that at low temperature, thin films exhibits amorphous nature. Also, it reduces the surface diffusion coefficient of the adsorbed vapor atoms and, thus, their reactivity, leading to the phase purity. On the other hand, a much higher temperature may result in loss of volatile elements. The dimension of plume can be controlled with the ambient gas pressure. As the oxygen gas pressure increases, the collisions between the plume and the oxygen gas increases as a result the plume dimension decreases and vice versa. Therefore, the effect of distance between target to substrate can be compensated using optimum oxygen gas pressure. The optimum oxygen pressure is important to maintain the stoichiometry. Higher oxygen pressure can increase the mobility of the species at the substrate surface, thus improving the annihilation of the induced defects. Also, it prevents the oxygen atoms of the thin film from leaving the substrate thus lowering the amount of vacancies and maintains the stoichiometry of the thin film. While, at a much lower pressure, ablated species having a higher kinetic energy impinge on the growing surface of thin film and generate defects beneath the surface layer via momentum transfer. It creates a larger amount of oxygen vacancies in the films.

Therefore, using small deviation around the best settings of the two dominant parameters of pressure and substrate temperature, the fine tuning experiment array has been formed and tabulated in Table 6. After performing these four fine tuning experiments, it is found that the first experiment listed in Table 6 results in single phase good quality NBT thin films with a dielectric constant of 735 and a dielectric loss of 0.07 at 1 kHz. Detailed structural, surface morphological, and dielectric investigation have been carried out on the sample used in the verification experiment.

3.2. Phase and structural analysis

NBT target and Pt coated Si substrate have been characterized using X-ray powder diffraction and NBT thin films have been characterized using grazing angle X-ray diffraction technique for phase and structure analysis. The XRD patterns for NBT target sintered at 1100 °C, Pt/Si substrate, and NBT thin films deposited using the best setting parameters of Taguchi are exhibited in Fig. 7.

The pattern for the NBT target can be indexed with a lattice parameter of 3.89 Å in a pseudo cubic structure. NBT thin films also exhibit a single phase perovskite structure. X-ray

Table. 5
Dominant parameters and their best setting for dielectric constant and dielectric loss.

Properties	Distance between target to substrate	Oxygen pressure	Substrate temperature	Laser fluence	Rate of repetition	Target	Annealing time
Dielectric	4 [cm]	0.1 [mbar]	650 [°C]	–	5 [Hz]	–	–
constant	14%	44%	23%	–	7%	–	–
Dielectric loss	–	0.3 [mbar]	650 [°C]	2 [J/cm^2]	5 [Hz]	–	30 min
	–	22%	30%	11%	19%	–	11%
Best setting	**4 cm**	**0.3 mbar**	**650 [°C]**	**2 [J/cm^2]**	**5 [Hz]**	**NBT**	**No annealing**

Table 6
Fine tuning experiments array.

Sample name	Distance between T–S [cm]	Pressure [mbar]	Substrate temperature [°C]	Fluence [J/cm^2]	Rate of repetition [Hz]	Target	Annealing
1	4	0.3	650	2	5	NBT	No
2	4	0.3	675	2	5	NBT	No
3	4	0.4	650	2	5	NBT	No
4	4	0.4	675	2	5	NBT	No

diffraction patterns have been indexed using JCPDS file (01–089–3109). When NBT thin films are characterized using simple powder diffraction technique, the intensity of NBT thin films pattern is dominated by the intensity of (111) platinum peak and (422) silicon peak obtained from the substrate due to which NBT peaks in the thin films are not visible significantly.

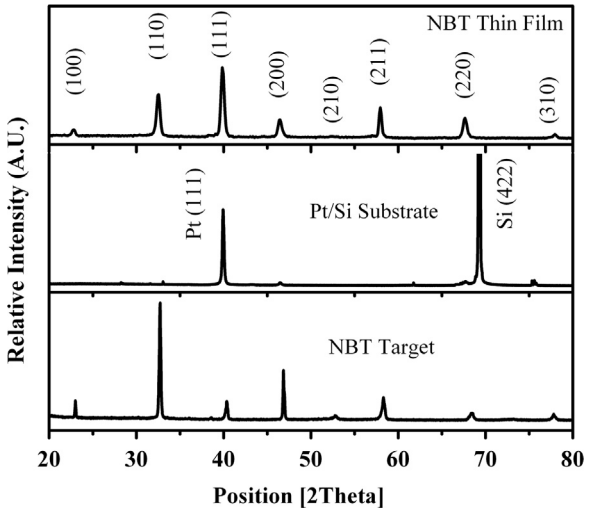

Fig. 7. X-ray diffraction pattern for NBT target, Pt/Si substrate and NBT thin films.

To remove or decrease the intensity of substrate peak, thin film grazing angle X-ray diffraction technique has been employed to characterize the NBT thin films. By changing grazing angle, the measured depth in a specimen can be controlled. In our case, NBT thin film is characterized using a 1/16 divergent slit, grazing angle of 0.5°, 0.1° step size and scan time per step at 10 s. It is observed that the intensity of the (111) peak increased in the thin film XRD patterns. The intensity ratio for the (110)/(111) for bulk NBT material is 4.76 whereas for NBT thin film is 0.65. Decrease in the intensity ratio for (110)/(111) peak implies that the NBT thin films exhibit preferred oriented along (111) direction.

3.3. Microstructure analysis and surface morphology

Microstructure analysis and surface morphology has been studied using field emission gun scanning electron microscopy (FEGSEM). Fig. 8(a) exhibits surface morphology of NBT thin film having a grainy structure. Grains size varies between 50 and 150 nm. Fig. 8(b) exhibits the cross-sectional SEM image of a NBT thin film showing different layers of Pt/TiO_2/SiO_2/Si substrate. Thickness of SiO_2, TiO_2, platinum and NBT thin film are around 500 nm, 40 nm, 100 nm and 400 nm respectively. Study of the surface topography of NBT thin film has been carried out using atomic force microscopy (AFM).

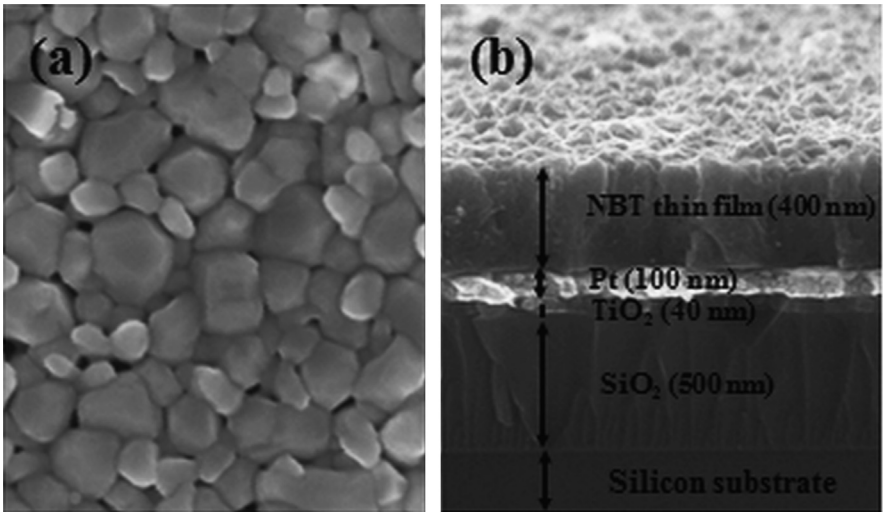

Fig. 8. (a) SEM image exhibiting surface morphology of NBT thin film. (b)Cross section SEM image of NBT thin films deposited on Pt coated Si substrate.

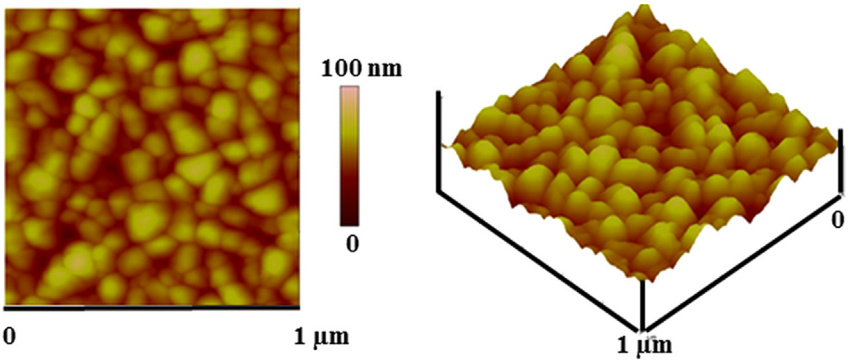

Fig. 9. 2d and 3d AFM image of NBT thin film deposited on Pt coated silicon substrate.

Fig. 9 exhibits 2d and 3d AFM image of NBT thin film featuring a grainy surface morphology like the SEM image. Section analysis of AFM image of NBT thin film yields 100 nm average grain size and root mean square roughness at around 5 nm.

3.4. Dielectric and ferroelectric properties

Dielectric constant and dielectric loss of the Au/NBT/Pt capacitor have been measured in the frequency range from 1 kHz to 1 MHz at room temperature. In Fig. 10, the dielectric constant decreases slowly from 735 to 241 over the frequency range from 1 kHz to 1 MHz. Dielectric loss is relatively stable over the frequency range from 1 kHz to 100 kHz and thereafter it increases at towards higher frequencies. The dielectric constant and dielectric loss at 1 kHz are observed to be 735 and 0.07 respectively.

Fig. 11 exhibits the electric polarization versus electric field response for Au/NBT/Pt like capacitor measured at room temperature by applying different voltage between 5 V and 25 V at 1 kHz. The value of remnant polarization (P_r) and coercive field (V_C) measured at voltage 25 V and at 1 kHz are 21.4 μC/cm^2 and 187 kV/cm respectively. The leakage current mechanism could be identified by plotting the leakage current density as a function of electric field as shown in Fig. 12. The leakage current density of NBT thin film is found to be 5.7×10^{-7} A/cm^2 at and above electric field 150 kV/cm which is better than those published in the literature [1],[2].

The values of remnant polarization of 21.4 (μC/cm^2), dielectric constant of 735 and dielectric loss of 0.07 at 1 kHz obtained in this work are comparable in both categories of chemical solution method and physical vapor deposition. The reason for these highest values can be attributed to high quality single phase thin films as observed in the XRD. The high coercive field is attributed to the presence of different size of randomly oriented grains in the plane of the film which results in broader grain boundaries and voids. Olysia m3 software has been used to quantify the grains and voids in the NBT thin films using SEM micrograph shown in Fig. 8 (a). It is observed that the average grain size is 96 nm. The grain size of minimum diameter is around 16 nm whereas maximum diameter of grain size is about 190 nm. The grain size distribution is shown in the pie chart in Fig. 13.

It is observed that majority of the grains vary in the size between 51 and 100 nm, while minorities of grains vary between 151 and 200 nm. Moreover, few voids are present at the junction of grain boundaries. Elsewhere, the grains are arranged in a compact manner. To align the grains in a particular direction as well as to increase the crystallinity without increasing deposition temperature of NBT thin films, it is proposed to study the NBT

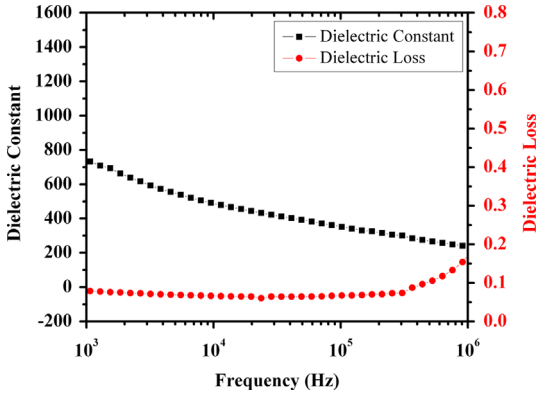

Fig. 10. Dielectric constant and dielectric loss of NBT thin film as a function of frequency.

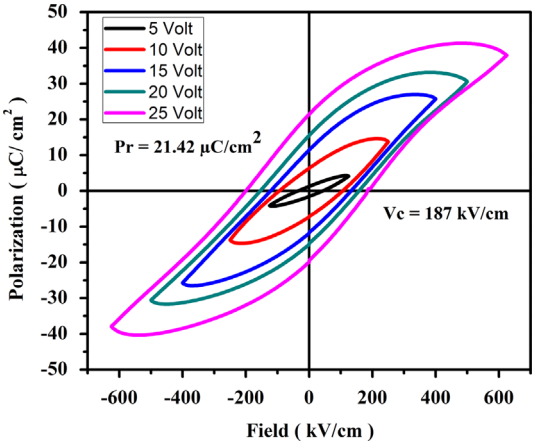

Fig. 11. Electric polarization versus electric field response for NBT thin film measured at room temperature by applying different voltage from 5–25 V.

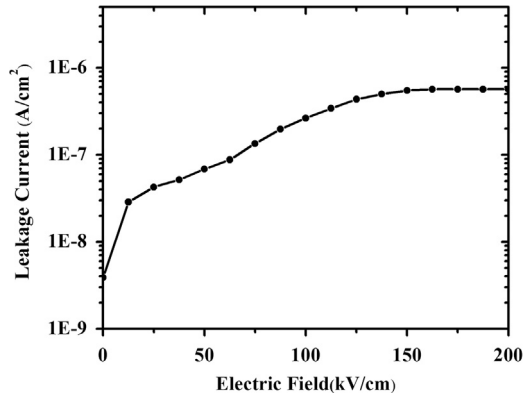

Fig. 12. Leakage current density curve of NBT thin films.

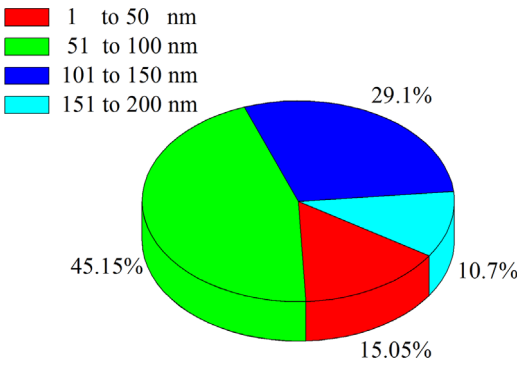

Fig. 13. Grain size distribution observed in SEM micrograph.

thin films using dielectric or conducting perovskite buffer layers with matched lattice constant.

4. Conclusions

Taguchi method has been adopted to optimize the PLD parameters for growing NBT thin films. Taguchi L_{18} array has been used to determine the effect of seven parameters on dielectric properties. The factor effect plots and ANOVA analysis identify the optimum parameters settings with which single phase NBT thin films can be obtained without excess Bi in the target. The results of the verification experiment with optimum settings exhibits the value of the dielectric constant of 735 and dielectric loss of 0.07 at 1 kHz. Ferroelectric study showed well saturated P–E loop upto electric field of 625 kV/cm with a remnant polarization of 21.4 $\mu C/cm^2$ and a coercive field of 187 kV/cm. These are the best reported values of dielectric constant and remanent polarization for NBT thin films. The reason for these highest values can be attributed to high quality single phase thin films as observed in the XRD. XRD clearly reveals (111) oriented NBT thin film without any secondary impurity phase. It is thus evident that if the parameters of PLD are optimized systematically then it is possible to obtain single phase NBT thin films without excess Bi in the target. However, though the Taguchi's approach simplifies the optimization procedure of PLD control parameters, it provides only the average quantitative effect of the process parameter on the desired properties. In the process, the technique yields the best properties for combination of optimum parameters. Precisely for this reason, effects of only dominant parameters on the quality of NBT thin films are predicted. From the materials point of view, in the case of NBT thin films, the Taguchi analysis established that only two parameters namely substrate temperature and oxygen pressure play a dominant role in deciding the quality of the thin films. This study opens the possibility for us and others to concentrate more time, efforts and resources in understanding the system with respect to variation in each of the two dominant parameters.

Acknowledgments

This work is supported by a generous research grant from Directorate of Extramural Research & Intellectual Property Rights, Defence Research and Development Organisation, New Delhi. Authors wish to thank Industrial Research and Consultancy Centre (IRCC) and Sophisticated Analytical Instrument Facility (SAIF) facility available at IIT Bombay.

References

[1] Z.H. Zhou, J.M. Xue, W.Z. Li, J. Wang, Ferroelectric and electrical behavior of $(Na_{0.5}Bi_{0.5})TiO_3$ thin films, Applied Physics Letters 85 (2004) 804–806.

[2] Z.H. Zhou, J.M. Xue, W.Z. Li, J. Wang, H. Zhu, J.M. Miao, Leakage current and charge carriers in $(Na_{0.5}Bi_{0.5})TiO_3$ thin film, Journal of Physics D: Applied Physics 38 (2005) 642–648.

[3] X.G. Tang, J. Wang, X.X. Wang, H.L. Chan, Preparation and electrical properties of highly (111)-oriented $(Na_{0.5}Bi_{0.5})TiO_3$ thin films by a sol–gel process, Chemistry of Materials 16 (2004) 5293–5296.

[4] C.Y. Kim, T. Sekino, Y. Yamamoto, K. Nihara, The synthesis of lead-free ferroelectric $Bi_{1/2}Na_{1/2}TiO_3$ thin film by solution-sol–gel method, Journal of Sol–Gel Science and Technology 33 (2005) 307–314.

[5] T. Yu, K.W. Kwok, H.L.W. Chan, Preparation and properties of sol–gel-derived $Bi_{0.5}Na_{0.5}TiO_3$ lead-free ferroelectric thin film, Thin Solid Films 515 (2007) 3563–3566.

[6] F. Remondiere, B. Malic, M. Kosec, J.P. Mercurio, Synthesis and crystallization pathway of $Na_{0.5}Bi_{0.5}TiO_3$ thin film obtained by a modified sol–gel route, Journal of the European Ceramic Society 27 (2007) 4363–4366.

[7] C.H. Yang, Z. Wang, Q.X. Li, J.H. Wang, Y.G. Yang, S.L. Gu, D. M. Yang, J.R. Han, Properties of $Na_{0.5}Bi_{0.5}TiO_3$ ferroelectric films prepared by chemical solution decomposition, Journal of Crystal Growth 284 (2005) 136–141.

[8] J.R. Duclere, C. Cibert, A. Boulle, V. Dorcet, P. Marchet, et al., Lead-free $Na_{0.5}Bi_{0.5}TiO_3$ ferroelectric thinfilms grown by pulsed laser deposition on epitaxial platinum bottom electrodes, Thin Solid Films 517 (2008) 592–597.

[9] M. Bousquet, J.R. Duclere, B. Gautier, C. Champeaux, A. Boulle, et al., Electrical properties of (110) epitaxial lead-free ferroelectric $Na_{0.5}Bi_{0.5}$-TiO_3 thin films grown by pulsed laser deposition: macroscopic and nanoscale data, Journal of Applied Physics 111 (2012) 104106–104119.

[10] S. Ando, K. Kanakahara, S. Okanura, T. Tsukamoto, Effect of laser energy density on the fabrication of $Ba_2NaNb_5O_{15}$ thin films by pulsed laser ablation, Japanese Journal of Applied Physics 36 (1997) 5925–5929.

[11] V. Bornand, S. Trolier-Mckinstry, Phase development in pulsed laser deposited $Pb[Yb_{1/2}Nb_{1/2}]O_3$–$PbTiO_3$ thin films, Thin Solid Films 370 (2000) 70–77.

[12] E.W. Kreutz, J. Gottmann, PLD of perovskite coatings for optoelectronics, microelectronics,and microtechnology, Journal of the European Ceramic Society 24 (2004) 979–984.

[13] J. Baek, J. Ma, M.F. Becker, J.W. Keto, D. Kovar, Correlations between optical properties, microstructure, and processing conditions of Aluminum nitride thin films fabricated by pulsed laser deposition, Thin Solid Films 515 (2007) 7096–7104.

[14] Y. Zhao, C. Chen, M. Song, J. Liu, Influence of the technical parameters on bioactive films deposited by pulsed laser, Surface Review and Letters 14 (2007) 283–291.

[15] W.J. Chou, C.H. Sun, G.P. Yu, J.H. Huang, Optimization of the deposition process of ZrN and TiN thin films on Si(100) using design of experiment method, Materials and Chemistry and Physics 82 (2003) 228–236.

[16] C.Y. Hsu, Y.C. Lina, L.M. Kaob, Y.C. Linc, Effect of deposition parameters and annealing temperature on the structure and properties of Al-doped ZnO thin films, Materials Chemistry and Physics 124 (2010) 330–335.

[17] T.C. Cheng, K.S. Yao, Y.H. Hsieh, L.L. Hsieh, C.Y. Chang, Optimizing preparation of the TiO_2 thin film reactor using the Taguchi method, Materials and Design 31 (2010) 1749–1751.

[18] M.S. Phadke, Quality Engineering Using Robust Design, PTR Prentice-Hall Inc., Englewood Cliffs, , New Jersey, 1989.